SECOND EUROPEAN CONFERENCE ON EARTHQUAKE ENGINEERING
AND SEISMOLOGY, ISTANBUL AUG. 25-29, 2014

STRUCTURAL HEALTH MONITORING OF A TALL BUILDING

Korkut Kaynardağ[1] and Serdar Soyöz[2]

ABSTRACT

Structural health monitoring techniques have been utilized to inspect the current conditions of structures, as well as their post-earthquake performances. The dynamic characteristics of a building, such as modal periods, shapes and damping ratios, can be obtained by analyzing the ambient vibration data. It is well-known that dynamic characteristics generated from the finite element model (FEM) and vibration data, even for the intact building, show remarkable differences. Assumptions made in the FEM are one of the main reasons for those differences.

To examine feasible solutions to such problems mentioned above, a twenty-six story, core-wall tall building in Istanbul was instrumented with a data acquisition system. Natural frequencies and mode shapes of the structure were determined by frequency domain decomposition method. In addition, identification of damping was performed due to the fact that damping ratio plays a significant role in the magnitude of inter-story drift during an earthquake. The FEM of the structure was constructed based on design drawings and updated to represent the real mode shapes and frequencies of the structure. By using the updated FEM with standard damping ratio in Turkish Earthquake Code and the identified damping ratio, seismic performance assessment of the building for a possible earthquake caused by the North Anatolian Fault was carried out.

INTRODUCTION

In recent decades, due to a lack of adequate construction sites, tall buildings have been the dominant means of accommodation and places of business in metropolises where economy and population grows fast. Compared to ordinary buildings, tall buildings are more densely populated, resulting in a bigger impact on the economy. In seismically prone areas, such as San Francisco, Tokyo and Istanbul, the safety of such buildings should be known prior to an earthquake and any damage due to the earthquake should be detected. To meet such necessities, tall building initiatives have been active especially in California to establish a framework for the selection of input motions, modeling approaches and performance criteria (Moehle, 2007).

Structural Health Monitoring (SHM) systems allow us to understand the dynamic characteristics of the buildings. SHM systems are based on data acquisition systems consisting of acceleration sensors and data recorders. Based on the ambient vibration data records, the dynamic characteristics of a building such as modal periods, shapes and damping ratios can be determined. Taking those characteristics into account, the existence of any damage and verification of design assumptions can be determined. In addition, the finite element model (FEM) of the building can be updated to represent the true behavior of the building. Californian seismic design guidelines recommend SHM systems to be installed on tall buildings as these systems make crucial contributions to the understanding of the dynamic behavior of buildings and enhance the capability of engineers for damage detection.

[1] Graduate Student, Bogazici University, Istanbul, korkut.kaynardag@boun.edu.tr
[2] Assistant Professor, Bogazici University, Istanbul, serdar.soyoz@boun.edu.tr

From the early 1980's, system identification with SHM systems has been applied in civil engineering. A comprehensive literature review on the vibration-based SHM was first presented by Doebling et al. (1996), summarizing hundreds of publications up to 1995. Recently, an updated review of the literature was presented by Sohn et al. (2003), summarizing publications from 1996 to 2001. In studies such as Beck and Jennings (1980); Yun and Shinozuka (1980); Safak (1991); Ghanem and Shinozuka (1995); Lus et al. (1999), structures were examined as a linear system and the modal parameters of this system were obtained in time or frequency domain. Moreover, earthquake responses of tall buildings have been investigated by using system identification techniques by Celebi and Safak (1991); Celebi et al., (2004). SHM was also employed for seismic performance evaluation in terms of inter-story drift ratios (Naeim, 1998; Celebi et al., 2004). Additionally, a FEM can be updated to acquire the value of structural parameters by minimizing the difference between the modal parameters obtained from FEM and from experimental data (Skolnik, 2006; Moaveni, 2009).

While vibration data can be utilized for damage detection, it can also be utilized to determine the real dynamic characteristics before any damage occurs. It is well-established that dynamic characteristics generated from FEM and vibration data, even for an intact building, show remarkable differences. The assumptions made for the FEM due the uncertainties in buildings are one of the main reasons of these differences as shown by Brownjohn et al. (2000). However, there are additional reasons causing such differences for tall buildings. Hence, the dynamic behaviors of tall buildings are even more unknown than those of ordinary buildings. For instance, higher modes dominate the behavior and the value of damping is less than that of ordinary buildings (Smith at al., 2010).

The ultimate goal of SHM is first to identify the structure accurately and then to predict its future performance i.e. reliability under operational or catastrophic events such as earthquakes. The current state-of-the-practice to estimate seismic reliability is to produce fragility curves of the buildings under numerous input motions so that the performance of a structure can be expressed in a quantitative way. Expression of seismic reliability in a quantitative manner is the only method for local and central authorities to make decisions and evaluations on the current state of structures. In order to express performance and reliability of the structures, fragility curves may be used as shown by Tantala and Deodatis (2002), Jayaram et al. (2012). Moreover, fragility curves of a structure can be derived from identified modal values as well as from FEM.

On the other hand, in some recent studies, it was illustrated that reliability of a bridge model exhibited differences between updated and non-updated models (Soyoz et al., 2010). Consequently, the determination of dynamic characteristics is essential in the sense that they define the actual seismic reliability of buildings.

In this research, a twenty-six story, core-wall tall building in Istanbul was instrumented with sixteen accelerometers. Following the installation and data acquisition, system identification was performed by the Frequency Domain Decomposition (FDD) method in order to obtain the natural frequencies and mode shapes of the building. These results were compared with the modal values obtained from the FEM of the building which is created according to design drawings. The effect of FEM updating with identified mode shapes and frequencies on the seismic demand of the structure is discussed in an article which is about the structure of this study by Kırkpınar at al. (2013). However, in this paper, the effect of damping is taken into consideration. It is observed that tall buildings have lower damping than ordinary buildings and overestimation of damping engenders higher accelerations and forces on structural elements. So, a final FEM with identified mode shapes and frequencies is generated. In addition to modal parameters obtained in the previous study, the damping ratio is also identified. Finally, seismic demand analyses were performed with 5% damping ratio which is allowed in the Turkish Earthquake Code and with the identified damping ratio in order to observe the performance of the building in a possible earthquake caused by the North Anatolian Fault. Probability density functions in terms of inter-story drift ratios are established in order to quantify the probability of failure under different ground motions. The result displays that damping is very significant in seismic demand of tall buildings.

BUILDING INFORMATION AND DATA ACQUISITION

The building in the study is one of the four high-rise buildings of an outstanding project which has been recently constructed in one of the financial centers of Istanbul's metropolitan region. Those

buildings are connected on the first stories by a large shopping mall. Therefore, the tributary area of the structure in the mall building and basement, and partially sorrounding structural system are also taken into consideration in addition to just the building itself. Figure 1 shows the outer view of the structure.

Figure 1. The structure monitored in the study.

The structural system of the high-rise building is a cast-in-situ reinforced concerete structure, consisting of two cores of structural walls in the center, and columns on the outer region. The structural plan is the same for all of residential floors in the tower and for almost all of the mall and basement floors. The height of each story, 3.5 meters, is also the same for the residential floors but they vary for the mall and the basement floors.

The instrumentation of the structure is carried out with sixteen accelerometers to measure the vibration response. The acceleromaters on the basement floor are set to a treshold value to capture the response of the building during an earthquake. Furthermore, internet access is provided to the data acquisition system, allowing remote control of the system and online data transfer through a computer or even a smart phone. Figure 2 shows the sensors located on a floor and the recorder located on the 12th story.

Figure 2. Acceleration sensors and data recorder.

Because of the fact that the number of channels of the recorder is limited up to sixteen, the location of sensors is adjusted to obtain the most of the dominant modes and to observe the mode shapes of those modes in an optimal fashion. For this purpose, the preliminary finite element analyses are performed and vibration measurements with temporary instruments are recorded. Based on them, the final configuration of the instrumented stories is determined as the -7th, 1st, 5th, 12th, 17th and 26th floors. For each story, acceleration responses in x and y directions are recorded at a position close to the centre. On the uppermost floor, an additional acceleromater is placed on the lateral y-direction, approximately 6 meters away from the centre, in order to observe the torsional modes of the structure. Furthermore, the floor at the foundation level is instrumented with an additional 3 acceleration sensors

for the purpose of measuring a rocking effect in case of an earthquake. Figure 3 shows the elevation and plan views of the sensor locations.

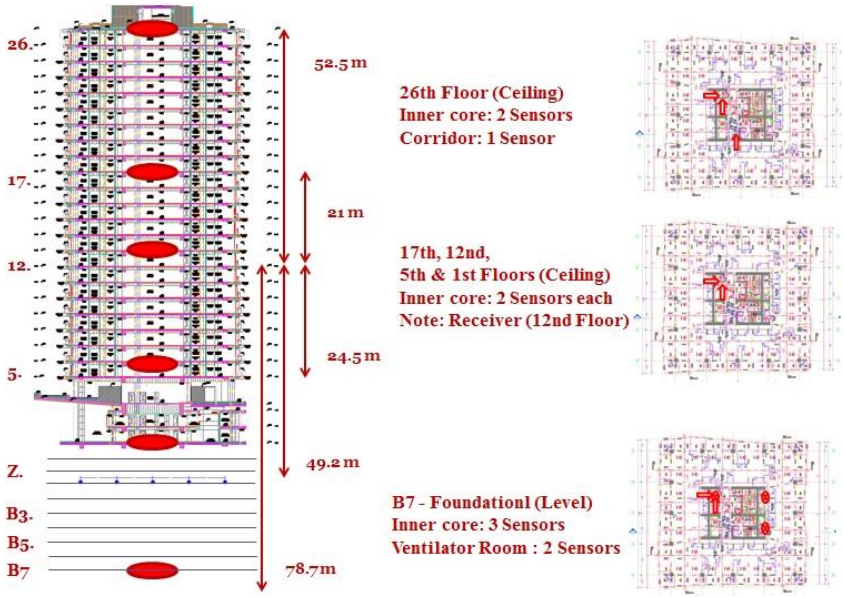

Figure 3. Sensor positions.

SYSTEM IDENTIFICATION

Ambient vibration measurements are collected for experimental modal analysis of the structure. According to the modal analysis results, it is recognized that the current system is capable of accurately measuring at least 4 modes of vibration in each lateral direction. Figure 4 displays the vibration measurements from 12th and 26th floors recorded instantaneously.

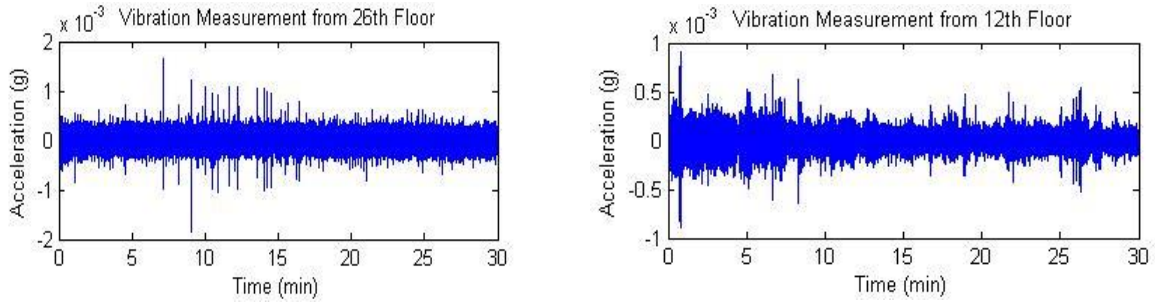

Figure 4. The vibration measurements from 12th and 26th floors recorded instantaneously.

In this study, the frequency domain decomposition (FDD) method which transforms the data in time domain to the frequency domain is used for system identification of modal frequencies and mode shapes (Brincker et al., 2001). This method is useful because it is not in need of any input and it is capable of identifying close modes. In this method, square matrices whose indices are the cross power spectral density of the data from two different sensors are generated for each frequency output. The singular value decomposition of those matrices gives spectral values and mode shapes for each matrix, therefore, for each frequency output discretized in the frequency domain.

Figure 5 demonstrates the cross power spectral density matrix where the peaks are the natural frequencies of the structure. From the figure, it is observed that the frequencies of the first, second, third, and fourth translational modes are 0.59, 2.25, 5.56, and 7.23 Hz, respectively in the y-direction as the result of modal identification. The other peaks represent the torsional modes identified, which are not considered in this study for FEM updating.

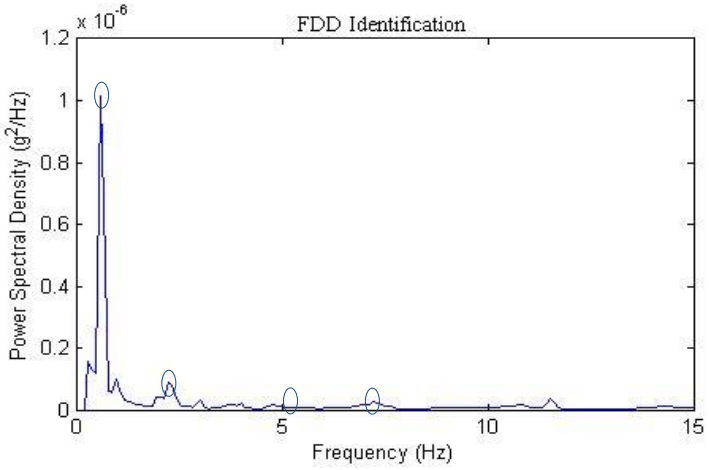

Figure 5. Identified natural frequencies.

After obtaining the cross power spectral density, the damping identification of the structure is performed. For this purpose, the impulse response function is generated by transforming the response of first mode in frequency domain to time domain. The level of decrease in the impulse response function gives the damping ratio and this decrease is an exponential decay unless there is any damage in the structure. Therefore, an exponential line is fitted to the peaks of each cycle in the impulse response and the damping ratio of the structure is identified as 1.94% from Figure 6. However, damping ratio is identified also according to a linear fit and it is calculated as 2.1%.

The damping ratio of the structures depends on numerous factors and it used to not be possible to know the exact damping ratio of a structure unless a full-scale experiment of the structure was performed. However, it has been recently possible to acquire the damping ratio of a particular building by the virtue of structural health monitoring techniques. It was examined that the damping ratio diminishes as the height of a structure increases. The damping measurements of several buildings with different heights are presented and a trend-line is obtained according to these measurements (Smith at al., 2010). Consequently, the damping ratio of the structure in interest is very close to that trend line.

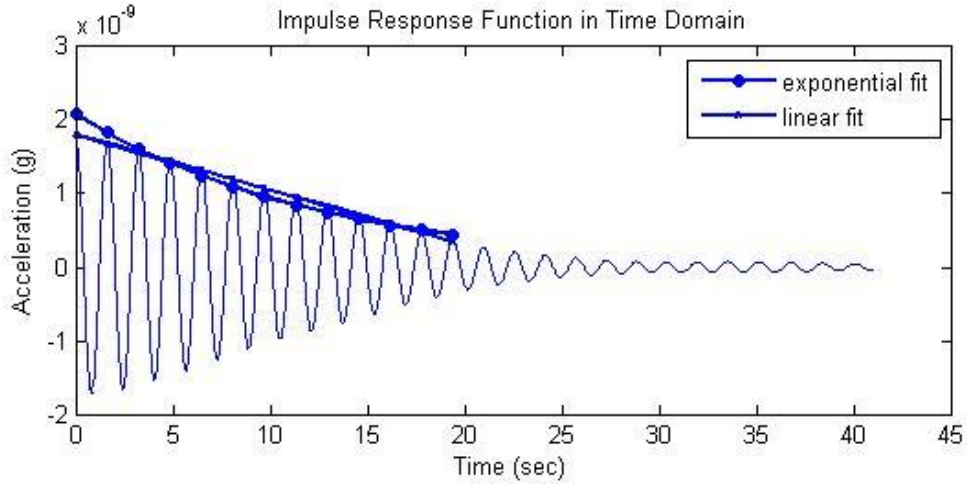

Figure 6. Impulse response function.

FINITE ELEMENT MODEL

Based on the design drawings and site investigations, a FEM is created in the SAP 2000 software platform. The effect of modelling structural walls by using shell elements and frame elements are discussed by Kırkpınar at al. (2013). Both of the approaches are tested and compared with each other in order to continue the updating procedure and the reliability estimation with the most suitable

approach. For this reason, prior to the decision of a conclusive model of the structure, models composed of shell elements with different meshing numbers are compared with the ones consisting of frame elements. It is concluded that use of frame elements accurately represents the optimal model with shell elements, therefore such approach can be used for forthcoming phases of the study.

In this study, the shear walls are modelled with frame elements instead of shell elements, therefore, the entire model consists solely of frame elements. Because of the fact that each part of the shear wall is constructed with a frame element, constraints are utilized to connect frame elements so that frame elements represent the behavior of the shear walls.

The structure consists of three different levels including the base, mall, and residential tower sections. The base section includes the stories under the ground level and it is rigidly connected with the foundation. Therefore, the model is fully restrained at its base. The mall section of the building is comprised of several stories which are surrounded by the overall mall structure in an irregular manner. By means of the identified mode shapes, it is known that there is considerable restraining effect from the surrounding structure around the mall and basement areas, because the part of the mode shapes around basement and shopping mall levels, especially basement level, are close to zero. However, discontinuity and complexity of many structural elements of the base and the mall floors caused difficulties in developing the FEM. Brownjohn et al. (2000) investigated the effect of modeling a high-rise building with different modeling approaches and three main approaches are concluded to simplify the unknown mass and stiffness contribution of the surrounding structure. One of the approaches includes the lateral restraints on the base and the mall stories. This approach is adopted in FEM because using springs is a suitable and efficient way to represent the stiffness contribution of the surrounding structure in the FEM. Springs are assigned on the first and fifth floors to represent the straining effect of the surrounding structure. Although the springs on these floors ignore the uncertainties on the other stories, they implicitly consider the effects of stiffness contributions coming from the instrumented floors.

Modulus of elasticity of the concrete is calculated with three different design codes called The American Concrete Institute (ACI) Code (2008), Eurocode 2 (2005) and Turkish Standards (TS-500). According to the concrete class used in the structure which is 50 MPa, initial elastic modulus of concrete for C50 is calculated as 33263 MPa, 36773 MPa, 36981 MPa respectively. ACI value is used for the modulus of elasticity of concrete. For cracked section inertias, 0.7 is used as a constant from ACI Code (2008).

To acquire the final model, the coefficients of springs are needed to be determined and the problem of uncertainty of modulus of elasticity should be solved. Moreover, there may be a decrease in stiffness of the structure due to several reasons, some of which may be additional mass and rigid end zones. Therefore, beside the coefficients of the springs, the modulus of elasticity is chosen as the third parameter which represents the overall stiffness of the structure besides the uncertainty of modulus of elasticity. Finally, in order to obtain the final model, the initial FEM is updated based on the modal values extracted from system identification by changing these three parameters.

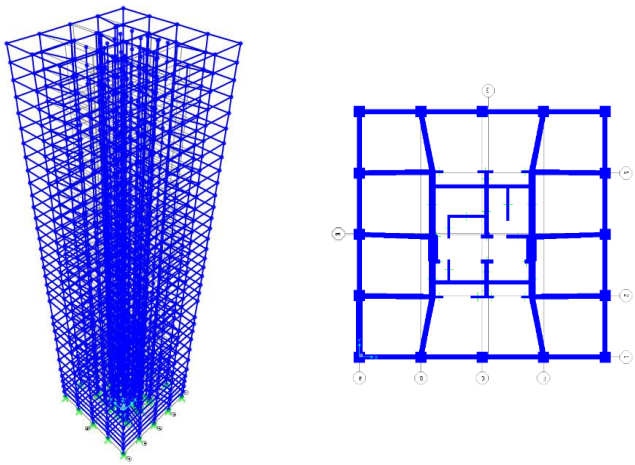

Figure 7. Finite Element Model in 3-D and top view.

FEM UPDATING

The FEM updating procedure was performed based on minimizing the difference between experimental and analytical modal values. For this purpose, a Matlab code which can automatically update the initial FEM by changing the structural parameters within determined values, and which gives the model values of each updated model was developed. The code compares modal outputs from each model with the identified modal parameters based on an error function to find the most optimal model. For this study, three different updating parameters mentioned above and 1000 different combinations of these parameters are utilized. Following the FEM updating procedure, modal frequencies and mode shapes which represent the ones generated from model identification are obtained. Equation 1 exhibits the objective function which quantifies the error between the simulations and the identification results.

$$E = \sum \left(k_i \cdot \left[\frac{(f_i^* - f_i)}{f_i^*} \right]^2 + h_i \cdot [1 - MAC_i]^2 \right) \quad (1)$$

Where,
i is mode number;
k_i is the weighing coefficient for i^{th} modal frequency;
h_i is the weighing coefficient for i^{th} modal assurance criteria;
f_i^* is the measured modal frequency of i^{th} mode;
f_i is the simulated modal frequency of i^{th} mode;
MAC_i is the modal assurance criteria for i^{th} mode shape.

Because of the fact that the primary modes have higher effects on the dynamic behavior of the structures, the objective function involves weighing coefficients to define the contribution of different modes. However, it is a well-known fact that higher modes play a significant role in the dynamic characteristics of tall buildings. The correlation between mode shapes obtained from system identifications and the simulations can be evaluated through the modal assurance criteria (MAC) of these modes. Consequently, the weighing of coefficients such as 0.80, 0.15, 0.05, and 0.01 are used respectively for comparison of the first, second, third, and fourth modal parameters. These coefficients are chosen according to the modal participation factors of corresponding modes and to the fact that the first modes respectively have major impacts on dynamic characteristics of the structure.

As a result of the minimization of the objective function for the first FEM, modulus of elasticity was identified as 19000 MPa. Moreover, the spring coefficients on the first and the fifth floor are identified as 2.5 and 5 GN/m, respectively. So, the final FEM with identified mode shapes and frequencies is produced by taking the effect of surrounding structure, uncertainty in modulus of elasticity and overall stiffness into account. These results indicate that the basement section restrains the structure remarkably so that the mode shapes are almost zero until ground level, and that the shopping mall doesn't give as much stiffness contribution as basement part does. In addition, the identified modulus of elasticity, which is lower than those of C50 concrete class calculated according to different design codes, demonstrates that the structure encounters a decrease in stiffness and this decrease may be derived from several reasons mentioned earlier, or from some other reasons. Table 1 shows the vibration frequencies of updated FEM and modal identification. Furthermore, Figure 8 exhibits the first, second, third and fourth mode shapes of identified, updated and non-updated FEM.

Table 1. Identified, non-updated and updated modal frequencies.

Mode Number	Frequencies of Vibration (Hz)		
	Updated FEM	Modal Identification	Non-updated FEM
1	0.59	0.59	0.44
2	2.48	2.25	1.90
3	4.92	5.26	4.43
4	6.87	7.23	6.97

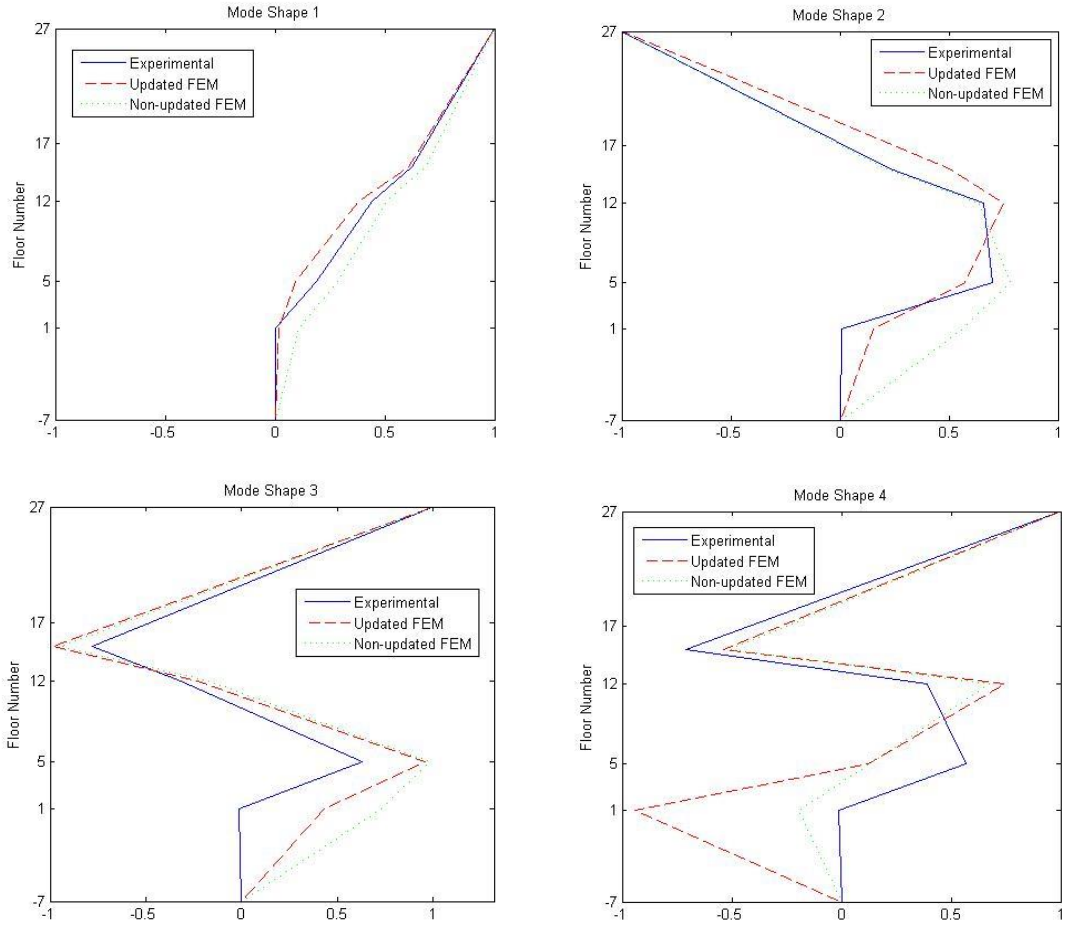

Figure 8. Experimental, updated and non-updated mode shapes

As a result, the modal parameters of first mode matched well with the identified modal parameters of first mode in the updated FEM due to the 80% weighing coefficient which is assigned to the comparison of the modal parameters of the first modes in the error function.

RELIABILITY ESTIMATION WITH THE UPDATED FEM

With the advent of sensor and computational technologies, SHM has experienced significant advance in the last 30 years. However, reliability estimation is rarely discussed in the literature from health monitoring perspectives. For this reason, further contribution regarding this subject is essential for a better comprehension of health monitoring results.

While trying to anticipate the seismic demand of the building, the North Anatolian Fault, which is the most important fault line in Anatolia, is considered as the main risk source. This fault line crosses Anatolia from one end to another and it is a very active seismic area with several major and lots of minor fault lines. Numerous historical records show that very destructive earthquakes were produced by this fault line. The last two of them were devastating Kocaeli (M=7.4) and Duzce (M=7.2) earthquakes which occurred in 1999. Following the East-West route, this fault line dives into Marmara Sea and continues to the West, getting as close as 10-20 km to Istanbul shores.

The building site is in the approximately 20-35 km north of the fault line. Therefore, twenty nine earthquake records are picked from PEER database to simulate the seismic demand on the building. These ground motions are selected according to their magnitude, distance and PGA values. These values are selected according to the characteristics of the expected earthquake in Istanbul which is approximated as a 7.5 magnitude, and the fault segment is 20-30 km away from the building site as suggested by Erdik et al. (2004). The building site is shown with a star on the map of the Marmara

segment of the North Anatolian Fault which is taken from the website of Republic of Turkey Prime Ministry Disaster and Emergency Management Presidency and can be seen in Figure 9 (www.afad.gov.tr).

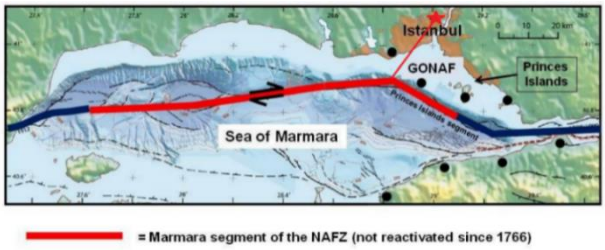

Figure 9. Marmara segment of the North Anatolian Fault Zone and the location of the building.

The response spectra of selected ground motions, their mean, the design spectrum in the Turkish Earthquake Code (2007) and two other alternative design spectra, which are suggested by Kandilli Observatory and Earthquake Research Institute (Koeri) and Gulkan and Kalkan (2004), are shown in Figure 10. This figure shows that different researchers and the current seismic design guideline of Turkey estimate different spectral acceleration values, and that the mean spectral acceleration value for the inputs picked for the study falls in between those of these studies. Therefore, at least for the current level of knowledge for the anticipated spectral acceleration values, the selected input motions give reasonable response values. Table 2 shows the input motions and their characteristics, maximum inter-story drift ratios of the building under the 5% and 1.94% damping ratios and increases in inter-story drift ratios.

Table 2. Earthquake records, maximum inter-story drift ratios and increases in inter-story drift ratios.

Earthquake Name	**Magnitude**	**Distance (km)**	**PGA (g)**	**Maximum Inter-story Drift Ratio (%)**		**Increase in Inter-story Drift Ratio (%)**
				%5 Damping Ratio	**1.94% Damping Ratio**	
Cape Mendocino (1)	7.1	18.5	0.549	0.33	0.35	6.06
Cape Mendocino (2)	7.1	33.8	0.229	0.048	0.69	43.75
Chi-Chi Taiwan (1)	7.6	26	0.639	0.43	0.62	44.19
Chi-Chi Taiwan (2)	7.6	43.4	0.712	0.30	0.50	66.67
Coalinga (1)	6.4	25.5	0.281	0.16	0.27	68.75
Coalinga (2)	6.4	29.9	0.282	0.35	0.38	8.57
Duzce,Tukey	7.1	17.6	0.822	0.44	0.54	22.73
Friuli, Italy	6.5	37.7	0.351	0.13	0.18	38.46
Imperial Valley (1)	6.5	10.4	0.315	0.41	0.49	19.51
Imperial Valley (2)	6.5	43.6	0.351	0.54	0.87	61.11
Irpinia, Italy (1)	6.5	32	0.358	0.38	0.20	10.53
Irpinia, Italy (2)	6.5	33	0.217	0.12	0.18	0.5
Kobe (1)	6.9	15.5	0.243	0.2	0.2	0
Kobe (2)	6.9	26.4	0.345	0.52	0.85	63.46
Kocaeli, Turkey (1)	7.4	17	0.244	0.16	0.23	27.78
Kocaeli, Turkey (2)	7.4	78.9	0.249	0.26	0.32	23.08
Landers (1)	7.3	21.2	0.417	0.32	0.38	18.75
Landers (2)	7.3	24.9	0.245	0.45	0.51	13.33
Loma Prieta (1)	6.9	16.9	0.638	0.36	0.46	27.78
Loma Prieta (2)	6.9	21.8	0.484	0.33	0.42	27.27
Northridge (1)	6.7	20.8	0.617	0.34	0.42	25.53
Northridge (2)	6.7	27.6	0.883	0.38	0.46	21.05
San Fernando (1)	6.6	20.3	0.366	0.14	0.17	21.43
San Fernando (2)	6.6	24.9	0.324	0.1	0.12	20
Superstition Hills (1)	6.7	24.4	0.408	0.044	0.12	34.09
Superstition Hills (2)	6.7	28.3	0.247	0.15	0.21	40
Tabas, Iran	7.4	17	0.406	0.27	0.39	44.44
Taiwan SMART1 (1)	6.4	64	0.254	0.18	0.22	22.22
Taiwan SMART1 (2)	7.3	39	0.242	0.19	0.29	52.63

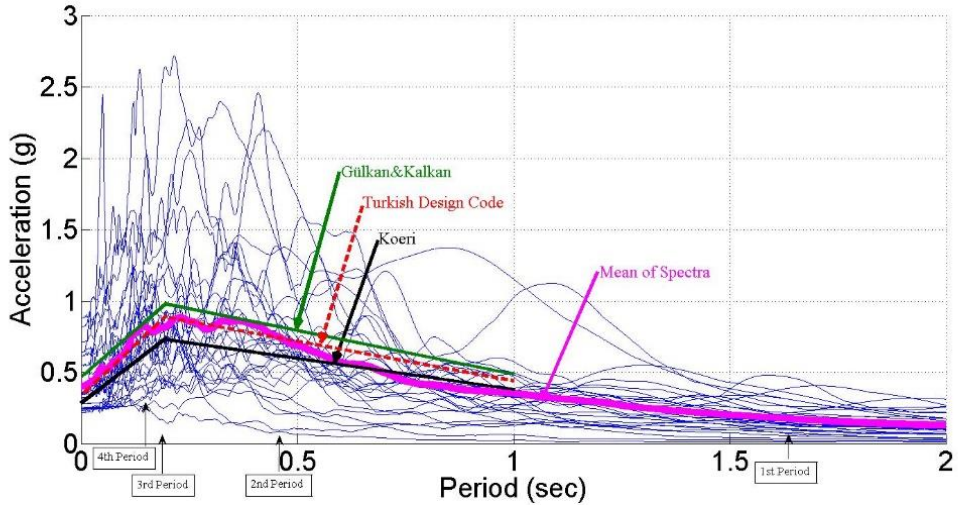

Figure 10. Response spectra and several design codes.

The maximum inter-story drift ratio values illustrate the effect of updating process. For 1.94% damping ratio, the biggest increases in maximum inter-story drift ratios between the non-updated and updated cases are in the records of Kobe (2), Cape Mendocino (2), Superstition Hills (2) and Imperial Valley (2). The increase in percentages of these earthquakes are 62.96%, 58.47%, 53.85% and 53.45% respectively. As an example, Figure 11 demonstrates the inter-story drift ratio time-history of Kobe (2) record for the 5% and 1.94% damping ratios.

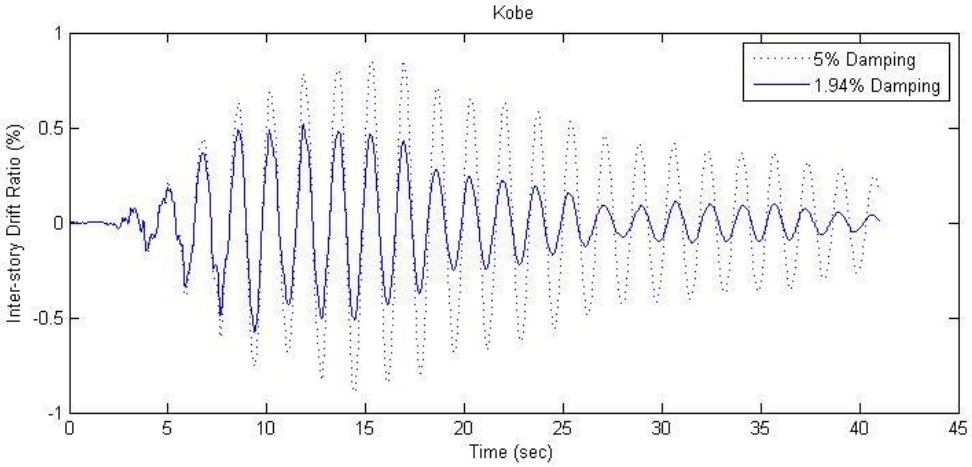

Figure 11. Maximum inter-story time history for Kobe (2).

In this study, the maximum inter-story drift ratio is determined as the damage indicator parameter. Twenty nine earthquake records are used as input data to perform linear time history analyses, and structural response is generated in terms of inter-story drift ratio time histories. These analysis results are used to construct probability density functions with log-normal distributions where random variables are the maximum inter-story drift ratios. The main purpose of this paper is to exhibit the impact of the damping ratio on the dynamic response of the structures. Therefore, this procedure is performed for 5% damping ratio which is allowed in the Turkish Earthquake Code and 1.94% which is the identified damping ratio. Figure 12 shows the probability densities as functions of maximum drift ratios. A threshold is set to 0.3% in order to see the effect of the identified damping ratio on inter-story drift ratio. The probability of damage is 12.62% for the 5% damping ratio whereas it is 62.45% for the 1.94% damping ratio. The huge increase in the probability of damage illustrates that the damping identification is very essential for tall buildings because of the fact that tall buildings have lower damping ratios than ordinary buildings.

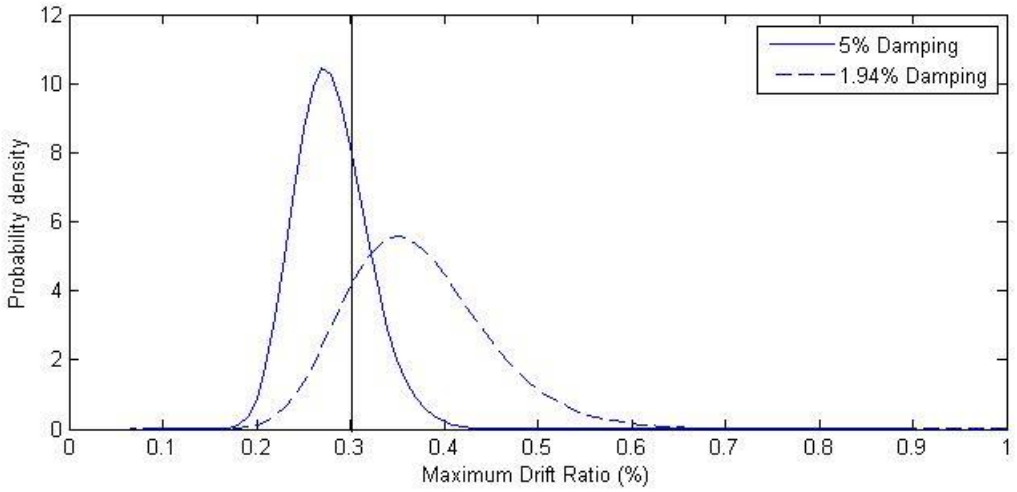

Figure 12. Probability densities as functions of maximum drift ratios

Moreover, even if the probability density functions demonstrate that the level of damage is not destructive, the cost of repairment may be too much or the building owner may not want any damage of his investment. Therefore, setting a maximum inter-story drift ratio plays a crucial role for such reasons. To emphasize this fact, two threshold ratios may be set as 0.2% and 0.5%. If the design of the structure is performed based on 0.5% maximum drift-ratio, Figure 12 shows that the structure with either of two damping ratios will not experience any damage. However, if the maximum inter-story drift ratio is set to 0.2% and if the design of structure is performed for this value, the structure will encounter damage during earthquakes regardless of its damping ratio.

CONCLUSION

In this study, system identification, finite element updating procedure and earthquake performance assessment of a tall building are performed. Frequency domain decomposition method is used for system identification. Based on identified mode shapes and frequencies, FEM which was conducted based on design drawings is updated to model the structure in interest with its current stiffness value and with the stiffness contributions from surrounding structure. It is found that the stiffness of the structure is lower than the stiffness obtained from FEM and there is a significant stiffness contribution from surrounding structure around the basement section.

The main purpose of the study is to investigate the effect of identified damping ratio of structure on seismic performance. So, the damping identification is performed based on the free decay of impulse response function. The damping ratio of the structure is found as 1.94% whereas the Turkish Earthquake Code allows 5% damping ratio for all structures. In order to examine the effect of different damping values, the seismic demands of the final FEM with the 5% and 1.94% damping ratios are evaluated in terms of inter-story drift ratios and inter-story drift ratio is chosen as the damage indicator. For this purpose, 29 earthquake motions are selected based on the characteristics of the expected earthquake in Istanbul. Based on results, log-normal probability density functions for 2 different damping ratios are produced. If a threshold value is set to 0.3% inter-story drift ratio, it is observed that the probability of damage for the structure in interest is 4.49 times more than one of the structure with the 5% damping. Therefore, the damping ratios of tall buildings should be examined carefully for seismic performance assessments because of the fact that such buildings usually have lower damping ratios than ordinary buildings.

In closing, if the damping ratio of the structure varies between 5% and 1.94%, the probability density functions illustrate that the probability of damage is concentrated between the 0.2% and 0.5% inter-story drift ratios. Therefore, to select a maximum inter-story drift ratio for design of structures has an essential effect on structural reliability.

REFERENCES

ACI Committee 318, 2008, "Building Code Requirements for Structural Concrete (ACI 318-08) and Commentary", *American Concrete Institute,* Farmington Hills, MI.

Beck J L and P C Jennings, 1980, "Structural Identification Using Linear Models and Earthquake Records", *Earthquake Engineering and Structural Dynamics,* Vol. 8, No. 2, pp. 145-160.

Brincker R, L Zhang and P Andersen, 2001, "Modal Identification of Output-Only Systems Using Frequency Domain Decomposition", *Smart Materials and Structures,* No. 12, pp. 441-445

Brownjohn J M W, T C Pan and X Y Deng, 2000, "Correlating Dynamic Characteristics from Field Measurements and Numerical Analysis of a High-Rise Building", *Earthquake Engineering and Structural Dynamics,* No. 29, pp. 523-543.

BS EN 1992-1-1 2005, "Eurocode 2: Design of Concrete Structures", *British Standard Institution,* London.

Celebi M and E Safak, 1991, "Seismic Response of Transamerica", *Journal of Structural Engineering,* Vol. 117, No. 8, pp. 2389-2425.

Celebi M, Sanli A, Sinclair M, Gallant S and Radulescu D (2004) "Real-time seismic monitoring needs of a building owner and the solution: A cooperative effort", *Earthquake Spectra,* 20:2, 333-346.

Doebling S W, Farrar C R, Prime M B and Shevitz D W (1996), Damage identification and health monitoring of structural and mechanical systems from changes in their vibration characteristics: A literature review, Los Alamos National Laboratory Report, LA-13070-MS.

Erdik M, M, Demircioglu K, Sesetyan E, Durukal and B, Siyahi, 2004, "Earthquake Hazard in Marmara Region, Turkey", *Soil Dynamics and Earthquake Engineering,* No. 24, pp. 605–631.

Ghanem R and M, Shinozuka, 1995, "Structural System Identification", *Journal of Engineering Mechanics,* Vol. 121, No. 2, pp. 255-273.

Guéguen P, C Michel and M Causse, 2012, "Seismic vulnerability assessment to slight damage based on experimental modal parameters", *Earthquake Engineering and Structural Dynamics,* No. 41, pp. 81–98.

Jayaram N, N Shome and M Rahnama, 2012, "Development Of Earthquake Damage Functions For Tall Buildings", *Earthquake Engineering and Structural Dynamics,* No. 41, pp. 1495–1514.

Kalkan E and P Gulkan, 2004, "Site-Dependent Spectra Derived from Ground Motion Records in Turkey", *Earthquake Spectra,* Vol. 20, No. 4, pp. 1111–1138

Kırkpınar E, Ozer E and Soyoz S (2013). Health monitoring and reliability estimation of a tall building, in *Proceedings of Second Conference - Smart Monitoring Assessment and Rehabilitation of Civil Structures,* September 8-11, 2013, Istanbul, Turkeymat

Moaveni B, Conte J P, and Hemez F M , 2009, "Uncertainity and Sensitivity Analysis of Damage Identification Results Obtained Using Finite Element Model Updating", Computer-Aided Civil and Infrastructure Engineering, 24, 320-334.

Moehle J P, 2007, "The Tall Building Initiative for Alternative Seismic Design" The Structural Design of Tall and Special Buildings, 16, 559-567.

Naeim F, 1998, "Performance of 20 Extensively-Instrumented Buildings During the 1994 Northrideg Earthquake" The Structural Design of Tall Buildings, 7, 179-194.

PEER Strong Motion Database, 2005, "The Pacific Earthquake Engineering Research" Center and the University of California.

SAP 2000, "Static and Dynamic Analysis of Structures Ultimate 15.1.0" Computers and Structures, Inc. 1995 University Ave. Berkeley, CA 94704.

Republic of Turkey Prime Ministry Disaster and Emergency Management Presidency Website: http://www.afad.gov.tr/TR/IcerikDetay.aspx?ID=192

Saito T, Morita K, Kashima T, and Hagesawa T, 2012 "Performance of High-Rise Buildings during the 2011 Great East Japan Earthquake" 15th World Conference on Earthquake Engineering, Lisboa, Portugal.

Skolnik D, Y Lei, E Yu and J W Wallace, 2006, "Identification, Model Updating, and Response Prediction of an Instrumented 15-Story Steel-Frame Building", *Earthquake Spectra,* Vol. 22, No. 3, pp. 781–802.

Smith R, Merello R and Willford M (2010) "Intrinsic and Supplementary Damping in Tall Buildings", *Structures and Buildings,* 163,111-118.

Sohn H, Farrar C R , Hemez F M , Shunk D D, Stinemates D W, Nadler B R, Czarnecki J J (2003), A review structural health monitoring literature: 1996-2001, Los Alamos National Laboratory Report, LA-13976-MS.

Soyoz S, Feng M Q , Shinozuka M (2010) "Structural Reliability Estimation with Vibration-based Identified Parameters" *Journal of Engineering Mechanics, ASCE,* 136 (1), 100-106.

Tantala M W, G Deodatis, 2002, "Development of Seismic Fragility Curves For Tall Buildings", *15th ASCE Engineering Mechanics Conference,* June 2-5, Columbia University, New York, NY

Turkish Standards Institute, "TS-500 Building Code Requirements for Structural Concrete", Ankara.

Turkish Standards Institute, 2007, "Turkish Earthquake Code", Ankara.